An NMR Study of the 7Fe-8S Ferredoxin from *Rhodopseudomonas palustris* and Reinterpretation of Data on Similar Systems[†]

Ivano Bertini,*,[‡] Alexander Dikiy,[‡] Claudio Luchinat,[§] Riccardo Macinai,[‡] Maria Silvia Viezzoli,[‡] and Massimo Vincenzini[||]

Department of Chemistry, University of Florence, Via Gino Capponi 7, 50121 Florence, Italy, Department of Soil Science and Plant Nutrition, University of Florence, P.le delle Cascine 28, 50144 Florence, Italy, and Research Center on Autotrophic Microorganisms, CNR, P.le delle Cascine 27, 50144 Florence, Italy

ABSTRACT: The oxidized 7Fe-8S ferredoxin from *Rhodopseudomonas palustris* is shown to possess a unique ^{1}H NMR spectrum displaying at least one hyperfine-shifted β-CH$_2$ signal for each cysteine bound to the [3Fe-4S] cluster. COSY and TOCSY spectra and 1- and 2-dimensional NOE experiments, in conjunction with a thorough reexamination of the ^{1}H NMR data on similar systems, permitted the sequential assignment of all of the cysteine β-CH$_2$ protons even in the absence of the amino acid sequence. The sequential assignment stems on the homology of the hyperfine shift pattern with those of other sequenced 7Fe-8S ferredoxins, which points to a substantial homology in tertiary structure. From the assignment, an analysis of the antiferromagnetic coupling in the [3Fe-4S] system was performed on the basis of a general model of exchange coupling. The NMR signal patterns of [3Fe-4S] clusters in both 3Fe-4S and 7Fe-8S ferredoxins have been discussed, and some correlations are proposed between signal patterns and the primary sequence.

Iron−sulfur proteins contain iron ions in the oxidation state either 2+ or 3+ bound to sulfide ions. They can be grouped according to their redox potentials as high-potential iron−sulfur proteins (HiPIPs) and ferredoxins. HiPIPs, with redox potentials higher than 90 mV (Meyer et al., 1983; Luchinat et al., 1994), contain a [4Fe-4S] core with formal charge 3+ or 2+. Ferredoxins have reduction potentials from 0 to −650 mV (Yoch & Carithers, 1979; Armstrong et al., 1988) and display a variety of iron−sulfur cores: $[2Fe-2S]^{2+/1+}$, $[3Fe-4S]^{1+/0}$, and $[4Fe-4S]^{2+/1+}$.

[3Fe-4S] clusters are encountered either alone (3Fe-4S proteins) or in association with [4Fe-4S] clusters (7Fe-8S proteins) (Berg & Holm, 1982; Thomson, 1985; Beinert, 1990; Holm, 1992; Cammack, 1992; Bertini et al., 1995). They usually display slightly negative reduction potentials.

The oxidized $[3Fe-4S]^+$ clusters have an $S = {}^1/_2$ ground state as a result of antiferromagnetic coupling among three ferric ions. Their ^{1}H nuclear magnetic resonance (NMR)[1] spectra show a variable number of hyperfine-shifted signals, mainly depending on whether the cluster belongs to a 3Fe-4S or 7Fe-8S protein (Moura et al., 1977, 1986, Sweeney,

1981; Day et al., 1988; Busse et al., 1992; Macedo et al., 1993a,b). In 3Fe-4S proteins, four hyperfine-shifted signals are observed downfield of the diamagnetic region. Two signals, which present a Curie-type temperature dependence (i.e., the shifts decrease with increasing temperature) and show dipolar connectivity between them, belong to the same cysteine of the [3Fe-4S] cluster. The other two signals have an anti-Curie temperature dependence (i.e., the shifts increase with increasing temperature) and do not show any reciprocal dipolar connectivity, each belonging to a different cysteine of the remaining two. This behavior has been accounted for by a simple magnetic coupling scheme in which two ferric ions are equivalent, with an antiferromagnetic coupling constant, *J*, between them larger than the other two coupling constants (Busse et al., 1992; Macedo et al., 1993a). The sequence-specific assignment is available in some cases (Macedo et al., 1993b; Donaire et al., 1994; Gorst et al., 1995). All four hyperfine-shifted signals assigned to cysteine β-CH$_2$ protons disappear upon reduction of the cluster (Macedo et al., 1993b), due to the much larger paramagnetism of the reduced $[3Fe-4S]^0$ species.

In oxidized 7Fe-8S ferredoxins, five downfield hyperfine-shifted signals are usually observed, three of which having an anti-Curie behavior and two a Curie behavior. Upon reduction of the [3Fe-4S] cluster, four out of these five signals disappear (Nagayama et al., 1983; Aono et al., 1996) with a behavior seemingly analogous to that of the 3Fe-4S proteins. However, oxidative destruction of the [4Fe-4S] cluster leaves only three hyperfine-shifted signals attributable to the oxidized [3Fe-4S] cluster (Nagayama & Ohmori, 1984;

* Address correspondence to this author at the Department of Chemistry, University of Florence, Via Gino Capponi, 7, 50121 Florence, Italy. Phone: (39) 55-275-7549. Fax: (39) 55-275-7555. E-mail: bertini@risc1.lrm.fi.cnr.it.
[‡] Department of Chemistry, University of Florence.
[§] Department of Soil Science and Plant Nutrition, University of Florence.
[||] Research Center on Autotrophic Microorganisms, CNR.

[1] Abbreviations: NMR, nuclear magnetic resonance; NOE, nuclear Overhauser effect; COSY, correlation spectroscopy; TOCSY, total correlation spectroscopy; NOESY, nuclear Overhauser spectroscopy; Fd, ferredoxin; Cys-(I, III, IV)[3], cysteines bound to the [3Fe-4S] cluster; Cys-(I, II, III, IV)[4], cysteines bound to the [4Fe-4S] cluster.

Nagayama et al., 1984). Based on these observations, three of the five hyperfine-shifted signals have been assigned to the [3Fe-4S] cluster and the remaining two to the [4Fe-4S] cluster (Nagayama & Ohmori, 1984; Cheng et al., 1990). A weak NOE between one signal of the first set and a signal of the second set is assigned to an intercluster NOE (Cheng et al., 1990; Bentrop et al., 1996; Aono et al., 1996). Of the three hyperfine-shifted signals assigned to the [3Fe-4S] cluster, two belong to the β-CH$_2$ group of one cysteine, and the third is a β-CH$_2$ proton of another cysteine. The ^{1}H NMR signals of the β-CH$_2$ protons from the third cysteine coordinated to the [3Fe-4S] cluster have never been observed. Most probably, they are hidden in the diamagnetic region of the spectrum.

In this work, we have studied the 7Fe-8S ferredoxin from *Rhodopseudomonas palustris*. The protein gives a ^{1}H NMR spectrum (Battistuzzi et al., 1995) which is similar to those already reported for other 7Fe-8S Fds in the low-field region of the spectrum (Nagayama et al., 1983, 1984; Nagayama & Ohmori, 1984; Johnson et al., 1987; Cheng et al., 1990, 1992; Bentrop et al., 1996; Aono et al., 1996). The present study has led to the assignment of a hyperfine-shifted signal in the upfield region of the ^{1}H NMR spectrum which is not present in the spectra of any other investigated 7Fe-8S Fds. This signal belongs to the [3Fe-4S] domain. Although this protein seems to have a unusually high molecular mass of 19 000 Da (Battistuzzi et al., 1995), and although the primary sequence is not known, the peculiar NMR spectra have motivated us to perform an extensive assignment of the cysteine protons to assess the inequivalence of the three iron ions, and then to interpret all the available NMR data on the basis of a general exchange-coupled Heisenberg model. The comparison with the NMR spectra of other 7Fe-8S proteins whose structures are available has lead to (i) the sequential assignment of the cysteine protons and (ii) the understanding of the general spectral features and their differentiation from those of the [3Fe-4S] clusters in 3Fe-4S proteins.

EXPERIMENTAL PROCEDURES

Rhodopseudomonas palustris strain 42 OL of the culture collection of the "Research Center on Autotrophic Microorganisms" was grown anaerobically in completely filled glass bottles under continuous illumination. Malate and ammonium sulfate were used as carbon and nitrogen sources, respectively. All chemicals used were of the best quality available. The protein was purified in the oxidized form as described earlier (Bartsch, 1971). Reduction of the protein was achieved by addition of 10-fold excess of sodium dithionite to the protein solution.

Samples for NMR spectroscopy (about 3 mM protein) were prepared in 50 mM phosphate buffer (either in H$_2$O or D$_2$O), pH 7.0. The NMR spectra were recorded using 500 DRX and 600 AMX Bruker spectrometers operating at 500.13 and 600.14 MHz Larmor frequencies, respectively. The spectra were calibrated by assigning the residual water signal a shift from TMS of 4.81 ppm at 298 K.

Longitudinal relaxation rates were measured using a nonselective inversion recovery pulse sequence (Vold et al., 1968). The T_1 values were obtained from a two-parameter fit of the data to an exponential recovery function as reported elsewhere (Bertini et al., 1996). The exponential behavior is verified within experimental error.

1D NOE spectra were recorded in the difference mode using previously described acquisition schemes (Banci et al., 1989; Dugad et al., 1990). Recycle delays and irradiation times were 220 and 100 ms, respectively, unless otherwise specified. A total of 64 000 scans were collected for each 1D NOE spectrum.

2D COSY spectra were recorded in the magnitude mode (Aue et al., 1976), with recycle delays varying from 100 to 300 ms. Magnitude mode spectra are more suitable in the presence of broad signals than their phase-sensitive analogues (Bertini et al., 1994; Bertini & Luchinat, 1996). A nonshifted squared sine bell window function was used to process the spectra. A 2D COSY spectrum aimed at detecting connectivities between β-CH$_2$ cysteine protons was recorded over 48 h, using 8K scans per experiment, 217 data points in the f_1 dimension, and 1K data points in the f_2 dimension.

The MLEV-17 spin lock sequence (Bax & Davis, 1985a) was used in TOCSY experiments. TOCSY (Bax & Davis, 1985b) and NOESY (Macura & Ernst, 1980) spectra were recorded in the phase-sensitive mode. Both NOESY and TOCSY experiments were preceded by a WEFT pulse sequence ($180-\tau-90$) to suppress signals of the protons which do not experience hyperfine interaction with the paramagnetic center and were optimized for the detection of the connectivities between the hyperfine-shifted signals and their neighbors (Chen et al., 1994; Banci et al., 1994; Luchinat & Piccioli, 1995). In TOCSY and NOESY experiments, the frequency carrier was shifted about 9 ppm downfield from the water signal to decrease the spectral window. The spectra were acquired with 512 data points in the f_1 dimension, from 256 to 1024 scans per experiment, and 2K data points in the f_2 dimension. In the NOESY experiments, the mixing times ranged from 4 to 40 ms. The spin lock time in 2D TOCSY experiments ranged from 2 to 10 ms. The data matrices were multiplied by a phase-shifted squared sine bell window function in both dimensions, prior to Fourier transformation.

The standard Bruker software package was used for data processing.

RESULTS AND DISCUSSION

The 298 K, 600 MHz ^{1}H NMR spectrum of the oxidized 7Fe-8S ferredoxin from *R. palustris* is shown in the upper trace of Figure 1. The downfield part of the spectrum clearly resembles the spectra of other investigated 7Fe-8S ferredoxins (Nagayama et al., 1983, 1984; Sweeney, 1981; Cheng et al., 1990; Aono et al., 1996), five signals (A−E) being shifted above 12 ppm. Three additional signals (F, G, H) are observed outside the diamagnetic envelope between 10 and 11 ppm. Furthermore, there is one signal (I) in the upfield region of the spectrum. The latter signal is not present in the spectra of any other 7Fe-8S Fds. The T_1 values of signals A−I range between 4 and 10 ms at 500 MHz (Table 1) and may be consistent with those of β-CH$_2$ protons of cysteines coordinated to the iron−sulfur clusters.

The temperature dependence of the nine shifted signals in the investigated temperature range is shown in Figure 2A. Two downfield-shifted signals (A and C) obey a marked (and a third signal, F, a slight) Curie-type temperature dependence, whereas all the other downfield-shifted signals reveal anti-Curie-type temperature dependence. The upfield-shifted signal I is the most sensitive to temperature, extrapolating
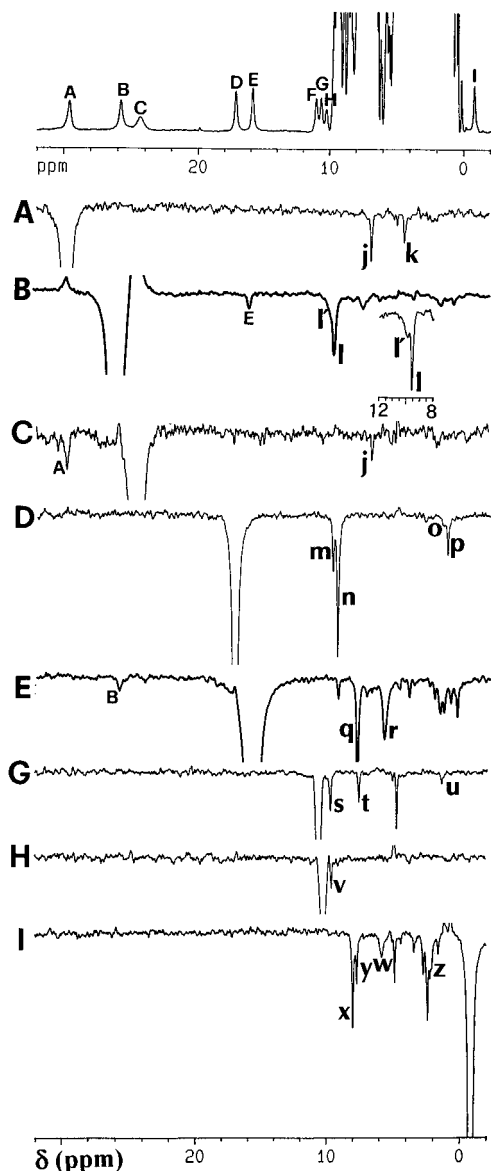
FIGURE 1: 298 K 600 MHz ^{1}H NMR spectra of the oxidized 7Fe-8S ferredoxin from *R. palustris* in 50 mM phosphate buffer in D$_2$O. The upper trace shows the reference spectrum. 1D NOE difference spectra, obtained upon saturation of the hyperfine-shifted signals, are shown on the other traces. Traces are labeled according to the saturated signal. Conditions: recycle time 220 ms, irradiation time 100 ms [80 and 40 ms, respectively, in the case of the NOEs on signal B performed at 298 K and 310 K (inset)].

sizably downfield (ca. 20 ppm) at infinite temperature, and thus obeying what has been termed a pseudo-Curie-type temperature dependence (Bertini et al., 1991; Banci et al., 1993). This behavior is typical of ligand nuclei experiencing contact shift from an iron ion which is exchange-coupled with an iron ion having larger spin.

The oxidized [3Fe-4S]$^+$ cluster has spin $^1/_2$ and thus the cysteine proton signals can experience any temperature dependence. On the contrary, the [4Fe-4S]$^{2+}$ cluster has spin zero, i.e., has a diamagnetic ground state and the cysteine proton signals can experience only anti-Curie behavior.

To perform the pairwise assignment of signals corresponding to the geminal β-CH$_2$ protons of the cysteines coordinated to the iron–sulfur clusters, 2D COSY and TOCSY spectra (Figure 3) were recorded. The two spectra may yield different information under extreme experimental conditions. In the COSY spectrum, scalar connectivities for signals D

(cross-peak 1), E (cross-peak 2), and I (cross-peaks 3 and 4) are observed. In the TOCSY map, besides the connectivities for signals D (cross-peak 1) and I (cross-peak 4), which were already observed in the COSY spectrum, two additional scalar connectivities for signals G (cross-peak 6) and H (cross-peak 7) are observed. In total, five out of the nine hyperfine-shifted signals A–I yield scalar connectivities. Both COSY and TOCSY experiments were acquired over long experimental times and under the best possible conditions to detect scalar connectivities between pairs of broad signals (see Experimental Procedures). Several processing parameters were tailored to optimize detection of cross-peaks within individual pairs. The signals of the present system display line widths ranging from 70 to 350 Hz. Signal C (350 Hz) is definitely too broad to give rise to scalar connectivity, while signals A and B (both about 130 Hz) might still be below the borderline. Apparently, their geminal partners are too broad to allow cross-peak detection. COSY experiments may provide cross-peaks under the occurrence of cross-correlation between proton–proton dipolar and proton–electron Curie relaxation (Bertini et al., 1993). Curie relaxation in the present system is estimated to be relatively small, and the above effect may be negligible. All five connectivities detected in COSY and TOCSY spectra are with proton signals in the diamagnetic region of the spectrum. The pairwise assignment of the β-CH$_2$ cysteine pairs involving signals D, E, G, and H is unequivocal. Discrimination between Hβ and Hα for the two scalar connectivities involving signal I, as well as the pairwise assignment for the remaining two cysteine β-CH$_2$ pairs, has been achieved through 1D and 2D NOE experiments performed at different temperatures. NOE experiments on paramagnetic systems are more challenging to perform than on diamagnetic analogues, as the NOEs can be much smaller due to paramagnetic T_1 shortening. On the other hand, and for the very same reason, spin diffusion effects are minimized and reliable distance information can be obtained (Bertini et al., 1989a; Banci et al., 1994).

298 K 600 MHz 1D NOE difference spectra obtained by saturating the hyperfine-shifted signals are shown in Figure 1. 1D NOE experiments at 291 K (data not shown), 2D NOESY at 284 K (Supporting Information, Figure S1), and 2D TOCSY experiments at 284 and 291 K (data not shown) have also been performed. Table 1 and Figure 2B summarize the results of the above experiments. The geminal partners of signals D, E, G, and H (signals n, r, s, and v) all show the expected anti-Curie temperature dependences and large line widths. Signals m and q, dipole–dipole coupled to signals D and E, respectively, and sharper than their β-CH$_2$ proton partners, also show anti-Curie temperature dependence and are tentatively assigned as the Hα protons of the cysteines having D–n and E–r as geminal pairs.

Several NOEs are observed by saturating the upfield-shifted signal I. Two of them (signals w and z) also give scalar connectivities with signal I (cross-peaks 3 and 4 in the COSY map). From all the signals giving NOE with signal I, only signal w has a sizable temperature dependence, which is of anti-Curie type. Signals I and w extrapolate approximately at the same positive chemical shift (ca. 20 ppm) at infinite temperature. The anti-Curie behavior of a signal hyperfine-shifted downfield is consistent with a pseudo-Curie behavior of a signal hyperfine-shifted upfield. Therefore, signal w, which is also broader than signal z, is

Table 1: Summary of the 1D NOE Experiments Performed on the Hyperfine-Shifted Signals of the Oxidized 7Fe-8S Fd from *R. palustris* at 291 and 298 K

| | 291 K | | 298 K | |
| | chem. shift of | chem. shift of | chem. shift of | chem. shift of |
signal	satur. signal (ppm)	obsd. NOE (ppm)	satur. signal (ppm) (T_1, ms)	obsd. NOE (ppm)
A	29.86	6.71(j), 4.26(k)	29.57 (4.3 ± 0.2)	6.71(j), 4.28(k)
B	25.57	9.40(l+l′)	25.78 (5.0 ± 0.2)	9.47(l+l′)
C	24.59	29.86(A)	24.37 (1.7 ± 0.1)	29.57(A), 6.71(j)
D	16.94	9.60(m), 9.23(n), 1.43(o), 1.14(p)	17.15 (6.2 ± 0.2)	9.69(m), 9.34(n), 1.43(o), 1.14(p)
E	15.67	7.99(q), 5.85(r)	15.87 (6.9 ± 0.1)	8.03(q), 6.04(r)
G	10.48	9.59(s), 7.62(t), 1.45(u)	10.63 (6.0 ± 0.2)	9.73(s), 7.61(t), 1.45(u)
H	10.17	9.46(v)	10.23 (4.1 ± 0.2)	9.59(v)
I	−1.24	5.48(w), 7.99(x), 7.67(y) 1.75(z)	−0.81 (10 ± 0.1)	5.78(w), 7.95(x), 7.66(y), 1.78(z)
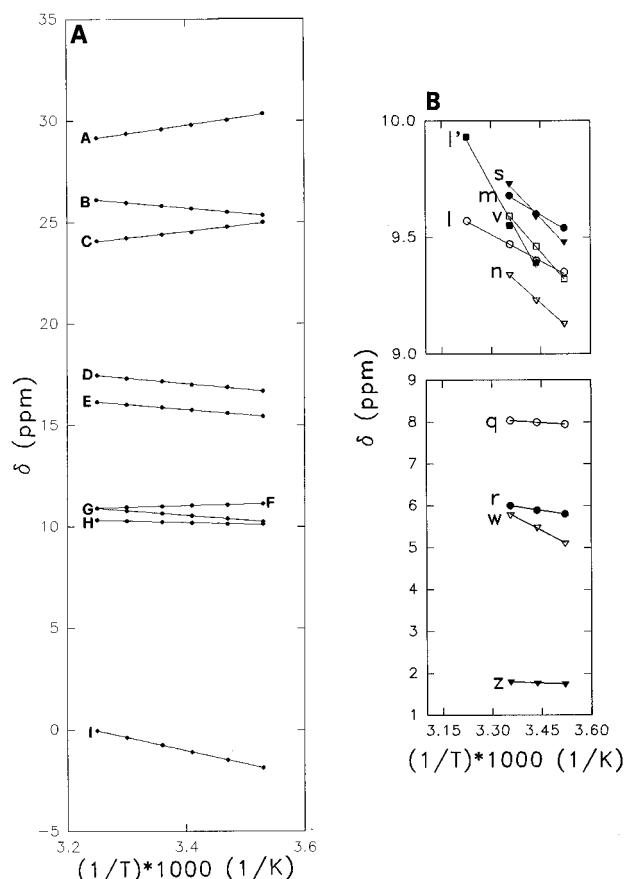
FIGURE 2: Temperature dependence of the ^{1}H NMR shifts of the signals corresponding to protons of the cysteine ligands of the oxidized 7Fe-8S ferredoxin from *R. palustris*: (A) hyperfine-shifted signals; (B) signals hidden in the diamagnetic region, obtained from 1D NOE and 2D spectra.

assigned as the geminal partner of signal I, and signal z as their Hα proton.

By saturating signal A, two signals, j and k, at 6.71 and 4.28 ppm, respectively, are observed. Both signals have essentially temperature-independent shifts. Moreover, the intensity of signal j substantially decreases with time in D$_2$O, thus indicating that it is due to a slowly exchangeable proton, possibly the backbone amide proton of the same cysteine. By saturation of signal C, an NOE is observed with signal A and with signal j (see above). The fact that the connectivity between A and C is observed only by saturating the latter and not by saturating the former is consistent with expectations, if their different T_1 values are considered. In fact, the observed steady-state NOE's are essentially proportional to the T_1 values, and the T_1 value of C is much shorter than the

T_1 value of A (see Table 1). Due to the observed dipolar connectivity between A and C, and their temperature dependence, we assign these signals as geminal β-CH$_2$ protons of the same cysteine.

By saturating signal B, an NOE with signal E and signal l at 9.47 ppm is observed. Another NOE to a broader signal l′ is observed as a shoulder of signal l. Signal l′ has been better resolved in the 1D NOE spectrum recorded at 310 K (Figure 1, inset of trace B). Both l and l′ display an anti-Curie-type temperature dependence, the latter being more sensitive to temperature. No other signal observed in the diamagnetic region of the 1D NOE spectrum upon saturation of B is temperature-dependent. Therefore, we assign signal l′ as the geminal β-CH$_2$ partner of signal B and l as their Hα proton. The dipolar connectivity between B and E should thus be between Hβ protons belonging to different cysteines.

Only very weak and temperature-independent NOEs are observed from signal F (not shown). Also in light of the results for the other eight hyperfine-shifted signals, signal F is obviously not due to a Hβ proton of a coordinated cysteine.

Summarizing, the combined use of 1D NOE and 2D COSY, TOCSY, and NOESY experiments together with the temperature dependence of the relevant signals allowed us to pairwise identify the β-CH$_2$ protons of all cysteines bound to the iron−sulfur clusters (Table 2). As mentioned before, the different temperature dependence of the hyperfine-shifted signals allows us to attribute two pairs of geminal protons (signals A−C and I−w) to the [3Fe-4S] cluster. At this stage, therefore, the β-CH$_2$ proton signals of two cysteines bound to the [3Fe-4S] cluster have been identified.

The protein is characterized by two reduction potentials of −260 and −560 mV (Battistuzzi et al., 1995) and, similarly to other 7Fe-8S proteins, can be reduced only at the first step. The semireduced protein contains a [3Fe-4S] cluster in a $S = 2$ ground state. The NMR signals of the β-CH$_2$ protons of the cysteines attached to the reduced [3Fe-4S] cluster have never been detected (Sweeney, 1981; Nagayama et al., 1983; Bentrop et al., 1996; Aono et al., 1996). Therefore, only the hyperfine-shifted signals corresponding to β-CH$_2$ protons of the cysteines attached to the [4Fe-4S] cluster should be in principle observed. Upon reduction, signals A, B, C, E, I, and H disappear (Figure 4). The reduction causes a slight shift of signal D. The ratio of the intensities of signal D to signal F in the semireduced state is close to unity, implying that signal E disappears from the downfield region of the spectrum rather than accidentally collapsing with signal D. This is confirmed by the difference NOE spectrum obtained by saturation of signal D in the
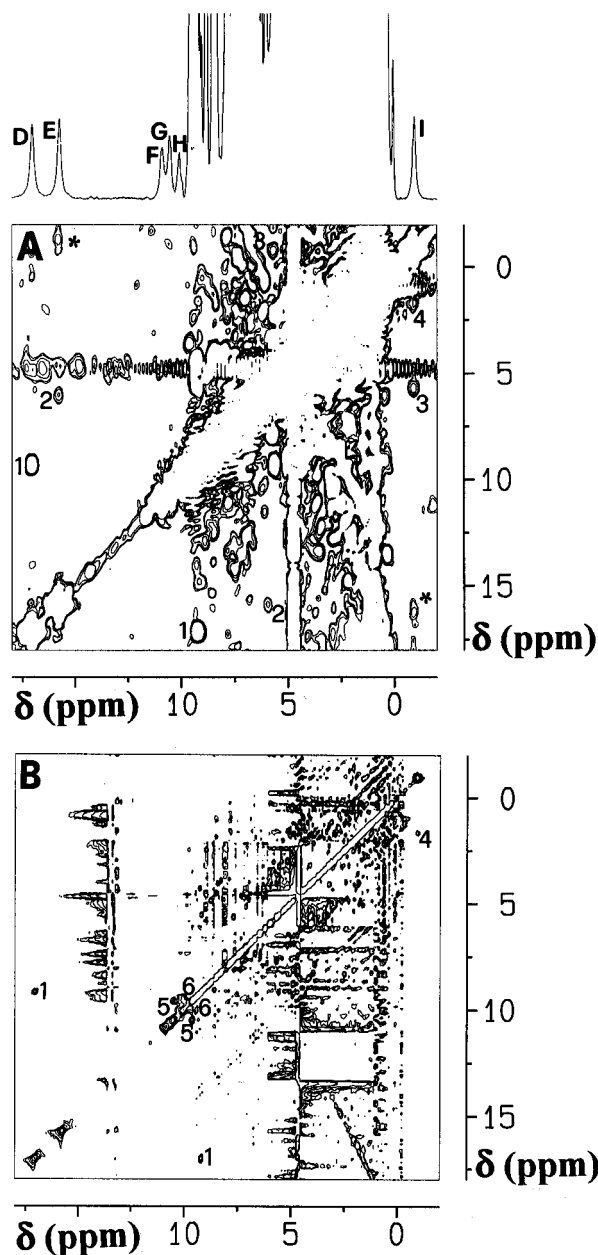
FIGURE 3: 298 K 500 MHz ^{1}H NMR 2D COSY (A) and TOCSY (B) spectra of the oxidized 7Fe-8S Ferredoxin from *R. palustris* in 50 mM phosphate buffer in D_2O. The TOCSY spectrum was acquired with a spin lock time of 8 ms. The cross-peak assignments are: (1) Hβ−Hβ' of Cys-II[4], (2) Hβ−Hβ' of Cys-III[4], (3) Hβ−Hβ' of Cys-I[3], (4) Hβ−Hα of Cys-I[3], (5) Hβ−Hβ' of Cys-I[4], (6) Hβ−Hβ' of Cys-IV[4]. The features marked with asterisks in (A) are artifacts that do not match the positions of E−I cross-peaks.

semireduced form (data not shown) which yields the pattern already observed for signal D in the oxidized state but not that observed for signal E. Obviously, too many signals disappear upon reduction. As was reported in the early literature (Nagayama & Ohmori, 1984; Nagayama et al., 1984), signals corresponding to signal B and to the A−C pair in our system survive oxidative degradation of the [4Fe-4S] cluster, while the other downfield-shifted signals disappear. This analogy allows us to assign the B−l' pair as due to the [3Fe-4S] cluster. Therefore, signals E and H must belong to the [4Fe-4S] domain even if they disappear upon reduction of the [3Fe-4S] cluster. In this frame, it is possible to assign the D−n, E−r, G−s, and H−v pairs as belonging to the cysteines coordinated to the [4Fe-4S] cluster, and the

Table 2: Pairwise Assignment[a] of β-CH$_2$ Protons of Cysteines Attached to Iron−Sulfur Clusters in the Oxidized 7Fe-8S Fd from *R. palustris* at 298 K

cysteine	signal	chem. shift (ppm)	T dependence[b]	cluster
cysteine-IV[3]	A	29.57	C	[3Fe-4S]
	C	24.37	C	
cysteine-III[3]	B	25.78	aC	[3Fe-4S]
	l'	9.47	aC	
cysteine-I[3]	I	-0.81	pC	[3Fe-4S]
	w	5.78	aC	
cysteine- II[4]	D	17.15	aC	[4Fe-4S]
	n	9.34	aC	
cysteine-III[4]	E	15.87	aC	[4Fe-4S]
	r	6.04	aC	
cysteine-I[4]	G	10.63	aC	[4Fe-4S]
	s	9.73	aC	
cysteine-IV[4]	H	10.23	aC	[4Fe-4S]
	v	9.59	aC	

[a] Chemical shifts reported at 298 K. [b] C, Curie; aC, anti-Curie; pC, pseudo-Curie type temperature dependence.
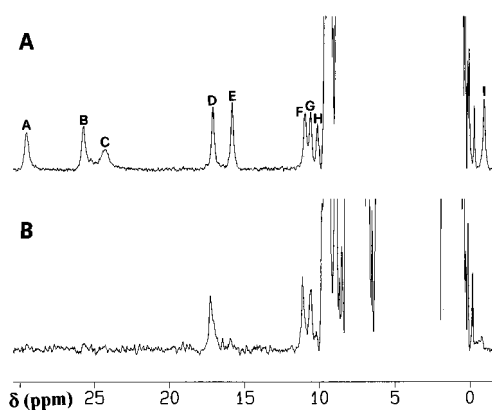

FIGURE 4: 298 K 500 MHz ^{1}H NMR spectra of the oxidized (A) and semireduced (B) 7Fe-8S ferredoxin from *R. palustris*.

A−C, B−l', and I−w pairs as belonging to the cysteines coordinated to the [3Fe-4S] cluster. The disappearance of signal H in the semireduced form could be tentatively explained by its shift inside the diamagnetic region. The disappearance of signals E can be accounted for by the fact that the corresponding proton is close to the [3Fe-4S] cluster, as proved by the intercluster NOE between signals B and E, and is broadened by the proximity with the reduced $S = 2$ paramagnetic center (Aono et al., 1996).

Sequential Assignment and Comparison with NMR Data on Other 3Fe-4S and 7Fe-8S Ferredoxins. Table 3 summarizes the NMR studies on 3Fe-4S and 7Fe-8S Fds reported in the literature. The simple comparison of the downfield-shifted regions of the NMR spectra of 3Fe-4S and 7Fe-8S proteins does not permit discrimination between the signals associated either with [3Fe-4S] or with [4Fe-4S] clusters. The downfield region of the 3Fe-4S Fds displays four hyperfine-shifted signals, whereas a larger number of signals is present in the same regions of the spectra of 7Fe-8S proteins. Therefore, one could expect that the additional signals in the case of the 7Fe-8S protein arise from the protons of the [4Fe-4S] domain. Among the downfield-shifted signals in the case of both 3Fe-4S and 7Fe-8S proteins, two signals reveal NOE connectivity to one another and obey a Curie-type temperature dependence. This observation permits the assignment of these protons as the geminal β-CH$_2$ pair of a cysteine bound to the [3Fe-4S]

Table 3: Summary of the Available NMR Data on 3Fe-4S and 7Fe-8S Ferredoxins

	βCH_2 Cys-I[3] aC	βCH_2 Cys-III[3] aC	βCH_2 Cys-IV[3] C	βCH_2 Cys-IV[4] aC	βCH_2 Cys-I[4] aC	βCH_2 Cys-II[4] aC	βCH_2 Cys-III[4] aC
D. gigas[a] (Macedo et al., 1993a)	~18, ~3.5	~15.2, ~8.5	29.2, 24.5				
Thermococcus litoralis[a] (Busseet al., 1992; Donaire et al., 1994)	17.4, 4.9	16.6, 8.1	29.2, 24.0				
P. furiosus[a] (Busse et al., 1992; Gorst et al., 1995)	(19.7, 17.1)[C]	14.3, 5.2	(23.6, 11.8)[aC]				
P. putida[b] (Cheng et al., 1990, 1992)	(0–10), (0–10)	21.8, (0–10)	31.8, 26.3[c]	9.8, 9.3[c,d]	9.8, 9.3[c,d]	17.3, (0–10)[c]	15.3, (0–10)
A. vinelandii[e] (Cheng et al., 1992)	(0–10), (0–10)	21.1, 8.6	32.2, 26.1[c]	(0–10), (0–10)	(0–10), (0–10)	16.9, 9.1[c]	15.2, 5.6
B. schlegelii[f] (Aono et al., 1996)	(0–9), (0–9)	18.3, 6.6	32.2, 23.4	10.35, ~9	11.1, 9.0	15.8, 9.7	15.9, 5.2
R. palustris[c,f]	−0.8, 5.8	25.8, 9.5	29.6, 24.4	10.2, 9.6	10.6, 9.7	17.15, 9.3	15.9, 6.0
D. ambivalens[a] (Bentrop et al., 1996)	20.0, 9.2	17.1, 7.5	21.7, 18.9	14.2, 7.9	10.9, 9.3	17.9, 9.2	14.0, 6.3
P. ovalis[c,g] (Nagayama et al., 1983)	(0–10), (0–10)	22.3, (0–10)	30.9, 25.7	10.5,[d] (0–10)	10.5,[d] (0–10)	17.7, (0–10)[h]	15.7, (0–10)[h]
M. smegmatis[c,g] (Nagayama et al., 1983)	(0–10), (0–10)	22.9, (0–10)	29.8, 21.5	11.0,[d] (0–10)	11.0,[d] (0–10)	17.1, (0–10)[h]	16.2, (0–10)[h]
T. thermophilus[c,g] (Nagayama et al., 1983)	(0–10), (0–10)	21.8, (0–10)	29.0, 21.1	11.1,[d] (0–10)	11.1,[d] (0–10)	17.4, (0–10)[h]	17.0, (0–10)[h]

[a] 303 K. [b] 281 K. [c] Sequence-specific assignment proposed in the present work. [d] Only one signal or one pair is observed. It is impossible to discriminate between Cys-IV[4] and Cys-I[4]. [e] 280 K. [f] 298 K. [g] 300 K. [h] The assignment to Cys-II[4] or Cys-III[4] could be reversed; C = Curie-type temperature dependence; aC = anti-Curie-type temperature dependence.

cluster. All other downfield-shifted signals show an anti-Curie-type temperature dependence. To assign these signals as belonging either to [3Fe-4S] or to [4Fe-4S] domains, combined spectral information from reduction and oxidative degradation is needed (see above) (Nagayama et al., 1983, 1984; Nagayama & Ohmori, 1984). These results unambiguously demonstrate that signals A, B, and C belong to protons of the [3Fe-4S] cluster domain, whereas signal D pertains to the [4Fe-4S] domain. Signal E can also be ascribed to the [4Fe-4S] cluster and can be recognized because of the intercluster NOE with signal B. This NOE has been observed in some other 7Fe-8S proteins (Cheng et al., 1990; Bentrop et al., 1996; Aono et al., 1996). The NMR signals corresponding to the remaining two cysteines bound to the [4Fe-4S] cluster in the other investigated 7Fe-8S proteins are either slightly shifted downfield from the diamagnetic region (11−10 ppm) or hidden inside the diamagnetic region. Some of these signals were identified in the case of *Pseudomonas putida* (Cheng et al., 1992), *Desulfurolobus ambivalens* (Bentrop et al., 1996), *Bacillus schlegelii* (Aono et al., 1996), *Pseudomonas ovalis* (Nagayama et al., 1983), *Mycobacterium smegmatis* (Nagayama et al., 1983), and *Thermus thermophilus* (Nagayama et al., 1983) 7Fe-8S Fds (see Table 3).

The amino acid sequences for the present and *D. ambivalens* 7Fe-8S Fds have not been determined. However, the homology of the hyperfine shift patterns with those of other sequenced 7Fe-8S ferredoxins suggests that a substantial homology in tertiary structure around the clusters occurs. The general cysteine binding scheme in 7Fe-8S systems is shown in Figure 5. With the reasonable assumption that the present protein conforms to a similar scheme, hints for the sequential assignment of the Cys β-CH$_2$ protons can be obtained by comparing the NMR data with analogous data, obtained for 3Fe-4S and 7Fe-8S ferredoxins, for which either the X-ray structure or a reasonable structural model is available. X-ray structures are reported for the 3Fe-4S Fd from *Desulfovibrio gigas* (Kissinger et al., 1991) and the 7Fe-8S from *Azotobacter vinelandii* (Stout, 1989). A structural model, starting from the X-ray structure of the latter protein, was built for *B. schlegelii* 7Fe-8S Fd (Aono et al., 1996), by introducing appropriate mutations and performing energy minimization. Analysis of the structural information
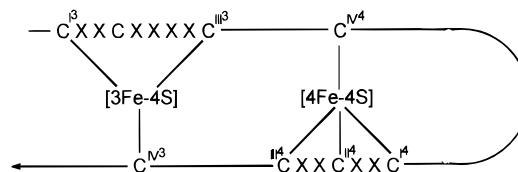

FIGURE 5: Schematic representation of a common cluster binding motif in 7Fe-8S ferredoxins (Cammack, 1992). The Roman numerals identify the commonly accepted order of the cysteines according to their binding to a certain iron in the cluster, and the superscript Arabic numerals specify the cluster type: 3 for [3Fe-4S] and 4 for [4Fe-4S] cluster.

together with NMR data leads to the sequential assignment of cluster-bound cysteines. As mentioned above, one intercluster dipolar connectivity was observed for some 7Fe-8S Fds. As it follows from the structures, the only cysteines which are close enough to give NOE to one another are Cys-III[3] and Cys-III[4] (where the roman and arabic numerals are defined in Figure 5). Therefore, signal B and its geminal proton correspond to β-CH$_2$ protons of Cys-III[3], whereas signal E with its geminal proton corresponds to β-CH$_2$ protons of Cys-III[4]. The other two hyperfine-shifted signals of the [3Fe-4S] cluster which give NOE to one another (signals A and C) could belong either to Cys-I[3] or to Cys-IV[3]. These signals have been assigned as belonging to Cys-IV[3] in *D. gigas* (Macedo et al., 1993a), *D. ambivalens* (Bentrop et al., 1996), and *B. schlegelii* (Aono et al., 1996). By analogy and on the basis of the similar pattern of 1D NOEs in the diamagnetic region, we maintain the same assignment. Signals I and w, belonging to the remaining cysteine ligand of the [3Fe-4S] cluster and observed only in the present case, are assigned as due to Cys-I[3]. The sequential assignment of the other three cysteines bound to the [4Fe-4S] cluster is a more difficult task since, as in most other cases, the signals fall in the diamagnetic region of the spectrum. An assignment can be performed, however, on the basis of the strict similarities of the relevant connectivities in the diamagnetic region for the present ferredoxin (NOEs from signals D, G, and H, Figure 1) with the corresponding connectivities in the analogous Fd from *B. schlegelii* (Aono et al., 1996). The complete assignment is reported in Table 2.

A further comment is due to the assignment of the upfield-shifted signal I to a β-CH$_2$ proton of a cysteine coordinated to the [3Fe-4S] cluster. This is a novel finding which sheds further light on the magnetic coupling operative in [3Fe-4S] clusters (see below). As the reliability of this assignment is crucial, we summarize again here the experimental evidence on which it is based: (i) signals I and w are strongly scalar coupled, the COSY cross-peak being easily detectable despite the short T_2 of the two signals; (ii) the T_2 values of I and w and the T_1 value of I are indicative of protons very close to the paramagnetic center; (iii) the strong temperature dependence of both I (pseudo-Curie) and w (anti-Curie), as well as their sizably downfield infinite temperature intercepts, is a clear indication of their experiencing strong hyperfine coupling with the [3Fe-4S] cluster, which can only occur through contact contributions. The shifts are only accidentally close to the diamagnetic values (5.7 and -0.8 ppm vs an expected diamagnetic value of $2.5-3$ ppm), around room temperature (see also Figure 7 below); (iv) signal I is strongly pH-dependent and disappears upon reduction, both features common to the other signals assigned to β-CH$_2$ protons of cysteines bound to the [3Fe-4S] cluster.

The information gained in the present work allows us to perform a systematic comparison of the data in Table 3 and to attempt some additional sequential assignments with respect to those already published.

The pair of cysteine β-CH$_2$ proton signals strongly shifted downfield and experiencing a Curie-type temperature dependence in the case of 7Fe-8S Fds from *A. vinelandii* and *P. putida* are assigned as due to Cys-IV[3] and not to Cys-I[3], on the basis of the similar behavior of analogous signals in 7Fe-8S Fds from *B. schlegelii* (Aono et al., 1996), *R. palustris*, and *D. ambivalens* (Bentrop et al., 1996). The downfield-shifted signals obeying a Curie behavior had been assigned as due to β-CH$_2$ protons of Cys-IV[3] also in the case of 3Fe-4S Fds from *D. gigas* (Macedo et al., 1993a) and *T. litoralis* (Busse et al., 1992; Donaire et al., 1994) [a different pattern is observed in the case of *P. furiosus* Fd (Busse et al., 1992; Gorst et al., 1995); see later]. Likewise, the signals corresponding to β-CH$_2$ protons of Cys-IV[3] in the spectra of the 7Fe-8S Fds from *P. ovalis*, *M. smegmatis*, and *T. thermophilus* are tentatively assigned on the basis of the strict similarity with the chemical shift values and line widths of the analogous signals in the spectra of 7Fe-8S Fds from *B. schlegelii* (Aono et al., 1996), *R. palustris*, *P. putida* (Cheng et al., 1992), and *A. vinelandii* (Cheng et al., 1992) even if the temperature dependence of their hyperfine shifts was not reported (Nagayama et al., 1983, 1984; Nagayama & Ohmori, 1984).

The ^{1}H NMR spectra of all investigated 7Fe-8S Fds [except for the one from *D. ambivalens* (Bentrop et al., 1996)] are characterized by the presence of three downfield-shifted signals with chemical shift values significantly larger than those of the other hyperfine-shifted signals. Two of these signals have been now assigned as due to Cys-IV[3]; the third one, in the case of 7Fe-8S Fds from *A. vinelandii* (Cheng et al., 1992), *P. putida* (Cheng et al., 1992), *B. schlegelii* (Aono et al., 1996), and *R. palustris*, has an anti-Curie temperature behavior and has been assigned as due to a Hβ proton of Cys-III[3] on the ground of the intercluster NOE with Cys-III[4]. As the downfield shift pattern is the same also for 7Fe-8S Fds from *P. ovalis*, *M. smegmatis*, and *T. thermophilus*, we also assign the corresponding third

downfield-shifted signal in the spectra of these proteins as due to one of the β-CH$_2$ protons of Cys-III[3].

Considering the available assignment of the β-CH$_2$ protons of the cysteines attached to the [4Fe-4S] cluster [again besides the 7Fe-8S Fd from *D. ambivalens* (Bentrop et al., 1996)], it can be easily noted that while two signals belonging to the two different cysteines are shifted downfield ($17-15$ ppm), the β-CH$_2$ proton signals of the other two cysteine fall either in the diamagnetic region or only slightly shifted downfield. The assignment of one of the signals from the former set as due to the Hβ proton of Cys-III[4] has been achieved through the intercluster NOE (see above). The other downfield-shifted signal from the first set has been assigned as due to one of the β-CH$_2$ proton's of Cys-II[4] in the case of the Fds from *B. schlegelii* (Aono et al., 1996) and *R. palustris*. By looking at the shift patterns of the other 7Fe-8S ferredoxins, it appears to be possible to group the β-CH$_2$ proton signals in two sets, according to the presence (Cys-II[4] and Cys-III[4]) or absence (Cys-IV[4] and Cys-I[4]) of one signal for each pair shifted above 15 ppm downfield. This observation allows us to assign the signals belonging to Hβ protons of Cys-II[4] in the case of 7Fe-8S Fds from *A. vinelandii* and *P. putida*, and to group the signals due to β-CH$_2$ protons of cysteines bound to the [4Fe-4S] cluster in the case of the 7Fe-8S Fds from *P. ovalis*, *M. smegmatis*, and *T. thermophilus* as shown in Table 3.

The information gained from the data and assignments reported in Table 3 can be summarized as follows:

(a) The spectral distribution of the NMR signals of β-CH$_2$ protons of the cysteines bound to the [3Fe-4S] cluster is different between 3Fe-4S and 7Fe-8S Fds. In the case of 3Fe-4S Fds, four signals (i.e., at least one proton signal of each cysteine bound to iron ions) are shifted downfield, whereas only three signals associated with the [3Fe-4S] domain of 7Fe-8S Fds are observed downfield. Two β-CH$_2$ proton signals of the third cysteine fall inside the diamagnetic region. Moreover, in the case of *R. palustris* Fd, one of the signals corresponding to the third cysteine was observed upfield.

(b) The pattern of the NMR signals corresponding to β-CH$_2$ protons of the cysteine associated with the [4Fe-4S] cluster is consistent for all studied 7Fe-8S Fds, excluding the Fd from *D. ambivalens*: two signals arising from two β-CH$_2$ protons of Cys-II[4] and Cys-III[4] are shifted well downfield, while signals corresponding to Cys-I[4] and Cys-IV[4] either are around 10 ppm or are hidden in the diamagnetic region.

(c) Concerning the cysteines bound to the [4Fe-4S] cluster in the 7Fe-8S Fds, it can be noted that the NMR shifts of β-CH$_2$ protons of Cys-I[4], Cys-II[4], and Cys-III[4] closely resemble the shifts of the corresponding signals in the 8Fe-8S Fds, while those of Cys-IV[4] seem to be somewhat different. In particular, the shifts of the two protons within the β-CH$_2$ pair of Cys-IV[4] are similar to one another in the 7Fe-8S Fds, while they are more spread in the 8Fe-8S Fds. This seems to be a general feature of 7Fe-8S Fds, probably connected to some structural motif that differentiates them from the 8Fe-8S Fds (see below).

(d) The 3Fe-4S Fd from *Pyrococcus furiosus* and the 7Fe-8S Fd from *D. ambivalens* reveal some NMR features which are different from those of other Fds. *P. furiosus* Fd displays a fifth signal at the borderline of the diamagnetic region, at variance with the four signals observed for the other 3Fe-

4S Fds. In the case of the 7Fe-8S Fd from *D. ambivalens*, the NMR pattern of the cysteine signals associated with the [3Fe-4S] cluster is more similar to that of 3Fe-4S Fds than to that of 7Fe-8S Fds. The shifts of the β-CH$_2$ protons of the cysteines bound to the [4Fe-4S] cluster in *D. ambivalens* are also different from the corresponding values for the cysteines attached to the [4Fe-4S] domain in the other 7Fe-8S Fds. They are more similar to those observed for cluster II of the 8Fe-8S Fds, including the shifts for the β-CH$_2$ protons of Cys-IV[4] (see above).

Some of these features can be tentatively explained by comparing the sequences of the 3Fe-4S, 4Fe-4S, 8Fe-8S, and 7Fe-8S Fds. While the sequential pattern of the first three cysteines bound to the cluster which is lacking in 3Fe-4S and in 4Fe-4S Fds (cluster II) is the same (C-X-X-C-X-X-C) for both 7Fe-8S and 8Fe-8S Fds, the pattern is different for the cysteines attached to cluster I in the four different Fd types. The pattern C[I]-X-X-C[II]-X-X-C[III] is maintained for 3Fe-4S, 4Fe-4S, and 8Fe-8S Fds (Cys-II is not bound to an iron ion in [3Fe-4S] cluster), whereas in the case of 7Fe-8S the pattern C[I]-X-X-C[II]-X-X-X-X-C[III] is often observed (Figure 5). This sequential asymmetry for the [3Fe-4S] domain in the 7Fe-8S Fds with respect to other Fd types may be the reason for the increased magnetic asymmetry evidenced by NMR, EPR (Glenn & Gold, 1985; Huynh et al., 1980; Kent et al., 1980), and Mössbauer investigations (Glenn & Gold, 1985; Huynh et al., 1980; Kent et al., 1980). This observation can be used to discuss the possible sequential motifs for 7Fe-8S Fds with unknown primary structure.

The sequential pattern for the [3Fe-4S] cluster observed for the 7Fe-8S Fd from *B. schlegelii* (C[I]-X-X-X-X-D-X-X-C[III]) (Aono et al., 1994) is different from those for [3Fe-4S] domain found for other 7Fe-8S Fds, although the number of residues between Cys-I[3] and Cys-III[3] is maintained (see above). Therefore, one could expect that the chemical shifts for the β-CH$_2$ protons of Cys-III[3] could be different with respect to the analogous shifts for other 7Fe-8S Fds. The data presented in Table 3 confirm this expectation: the hyperfine shift of one β-CH$_2$ proton of Cys-III[3] is on average 5 ppm more upfield than the same protons in other 7Fe-8S Fds. The similarity of the NMR pattern of the β-CH$_2$ protons of 7Fe-8S Fd from *D. ambivalens* to those of 8Fe-8S Fds could indicate that the sequence of this protein is more similar to those of 8Fe-8S Fds, rather than 7Fe-8S Fds. Indeed, preliminary sequential information for 7Fe-8S Fd from *D. ambivalens* gives the following pattern for cluster I: C[I]-X-X-D-X-X-C[III] (Bentrop et al., 1996), which has the same length as for the 8Fe-8S ferredoxins. The similarity of the NMR data obtained for the 7Fe-8S Fd from *R. palustris* with those observed for other 7Fe-8S Fds could indicate that the sequence of the present Fd is similar to those reported for most of the other 7Fe-8S ferredoxins.

NMR pH Dependence. The pH dependencies of the hyperfine-shifted signals of the oxidized *R. palustris* 7Fe-8S Fd are shown in Figure 6. The best fitting of the experimental points using a unique pK_a for all signals provide a pK_a value of 5.4 ± 0.2. As the standard deviation is very small, it is reasonable to assume that all hyperfine shifts are titrated with the same pK_a value.

The obtained pK_a value for the hyperfine-shifted signals is similar to those observed for the analogous signals in 7Fe-8S Fds from *A. vinelandii* (pK_a 5.4) (Cheng et al., 1990)
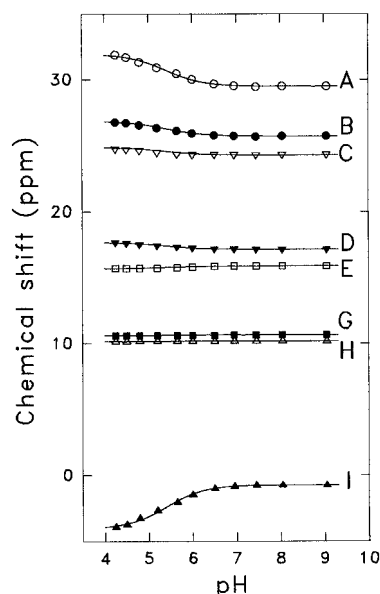

FIGURE 6: pH dependence of the ^{1}H NMR shifts of the hyperfine-shifted signals of the oxidized 7Fe-8S ferredoxin from *R. palustris*.

and *P. putida* (pK_a 5.6) (Cheng et al., 1990). The pK_a of 5.4 observed in the present case, in analogy with the mentioned ferredoxins, probably corresponds to titration of the Asp-15 residue (numbering of the 7Fe-8S Fd from *A. vinelandii*).

Comments on the J Values in the Oxidized [3Fe-4S] Cluster. The present 7Fe-8S system has the unique and peculiar feature of displaying an *upfield-shifted* cysteine β-CH$_2$ proton, assigned as arising from the [3Fe-4S] cluster. By looking at Table 3, it can be observed that the magnetic exchange coupling scheme in the [3Fe-4S] cluster of 7Fe-8S ferredoxins must be less symmetric than in single-cluster 3Fe-4S proteins. Indeed, in the latter, one β-CH$_2$ proton for each of the two cysteines experiencing anti-Curie behavior is observed in the downfield region of the ^{1}H NMR spectrum, indicating a substantial equivalence of the two corresponding iron ions. Therefore, the two-Curie/four-anti-Curie pattern of the cysteine β-CH$_2$ proton shifts could be accounted for by using a symmetric coupling scheme where the J values between one spin (S_1) and the other two (J_{12} and J_{13}) were equal, and the third J value (J_{23}) was larger than the other two. In this way, the eigenfunctions could be described in terms of a subspin S_{23} ($=S_2 + S_3$) antiferromagnetically coupled to the third spin, S_1, $|S_{23}, S_1\rangle$, and the ground state was made up by a $|2, 5/2\rangle$ function. Only a modest (within ±10%) difference between J_{23} and $J_{12} = J_{13}$ is enough to account for the experimental $1/T$ dependence (Busse et al., 1992; Macedo et al., 1993a).

This description constitutes a more crude approximation for the less symmetric [3Fe-4S] clusters in 7Fe-8S proteins. In these proteins, one of the two anti-Curie β-CH$_2$ pairs is much less shifted than the other, and either lies in the diamagnetic region or appears in the high-field part of the spectrum. To treat this case appropriately, we should then resort to numerical solutions of the general Hamiltonian:

$$H = J_{12}S_1S_2 + J_{13}S_1S_3 + J_{23}S_2S_3 \qquad (1)$$

for which we have adapted a computer program developed by us for general numerical solutions of the [4Fe-4S] coupling scheme. The $S_1 = 5/2$, $S_2 = 5/2$, $S_3 = 5/2$ coupled
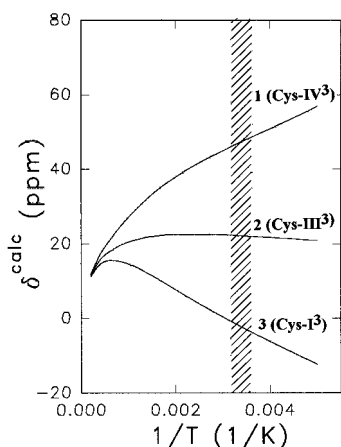
FIGURE 7: Calculated temperature dependences of the shifts of the ^{1}H NMR signals of the cysteine β-CH$_2$ protons (averaged for each pair) bound to the [3Fe-4S] cluster in 7Fe-8S ferredoxins. The plots were obtained using the following set of J values: $J_{12} = 285$ cm^{-1}, $J_{13} = 300$ cm^{-1}, $J_{23} = 320$ cm^{-1}. The dashed region corresponds to the temperature range of the experiments. The iron ion numbering used in the calculations is also shown, together with the sequential cysteine numbering in the present system.

system can be described by eigenfunctions that are linear combination of $|M_{S1}, M_{S2}, M_{S3}\rangle$ eigenfunctions of the uncoupled system (Bertini et al., 1989b; Banci et al., 1991). The problem reduces to diagonalization of a $[(2S_1 + 1)(2S_2 + 1)(2S_3 + 1)]^2 = 216 \times 216$ matrix. The latter can be further reduced in blocks, each having the same ΣM_{Si}, and the largest (27×27) being the one for which $\Sigma M_{Si} = \frac{1}{2}$.

Except for the situation of three equal J values, the ground state is nondegenerate and well separated from the first excited state (see Supporting Information). This justifies the experimental observation that room temperature NMR data still contain information on the order of the J values (see below). Using Hamiltonian (1), we can attempt to reproduce the experimental hyperfine shifts. The hyperfine shifts, assumed mainly contact in origin, for a β-CH$_2$ pair of a cysteine bound to iron i depend on the $\langle S_{iz} \rangle$ value for that iron according to eq 2:

$$\delta^{\text{hyp}} = (A/h)\langle S_{iz} \rangle \qquad (2)$$

where A/h is the hyperfine coupling constant that would be observed in an uncoupled system. The shifts of the three pairs of cysteine β-CH$_2$ protons in the coupled system are thus differentiated by the different values of $\langle S_{iz} \rangle$. The shifts within each pair are then further differentiated by the values of the two M$-$S$-$C$-$H dihedral angles. We chose 1 MHz as a starting value for A/h (Bertini et al., 1995). Such a value accounts for the 200$-$300 ppm downfield shifts observed in rubredoxin (Werth et al., 1987). To obtain shifts in the -10 to 40 ppm range in the coupled system, an average value of J of about 300 cm^{-1} is needed (Macedo et al., 1993a; Busse et al., 1992; Bertini et al., 1995). By using these starting values, $1/T$ plots for the three β-CH$_2$ pairs can be generated. It appears that a qualitative agreement with the (average) hyperfine shifts of the three pairs (Figure 7) is observed with the following set of J values: $J_{12} = 285$ cm^{-1}, $J_{13} = 300$ cm^{-1}, and $J_{23} = 320$ cm^{-1}. In the present system, iron 1 is the one coordinated to Cys-IV^3, iron 2 to Cys-III^3, and iron 3 to Cys-I^3 (Figure 7). The present finding and theoretical reconsideration of hyperfine shifts asymmetry in [3Fe-4S] clusters are in line with previous observation of

hyperfine-coupling asymmetry in low-temperature Möss-bauer spectra of several 7Fe-8S ferredoxins (Glenn & Gold, 1985; Huynh et al., 1980; Kent et al., 1980).

It should be pointed out that the slight upfield shift of one of the protons bound to iron 3 (Cys-I^3) could be easily lost if the difference between J_{12} and J_{13} is slightly reduced. The corresponding β-CH$_2$ protons are not observed in other 7Fe-8S systems because they lie in the diamagnetic region. The slightly larger hyperfine shift asymmetry in the present 7Fe-8S system is, therefore, hardly related to significant structural differences.

CONCLUDING REMARKS

A detailed analysis of the 7Fe-8S ferredoxin from *R. palustris*, even in the absence of knowledge of the primary structure, has allowed us to observe for the first time all geminal protons of the cysteines bound to the seven iron ions. Exploitation of literature data on analogous proteins and theoretical prediction based on a exchange-coupled Heisenberg model have permitted the pairwise assignment of the β-CH$_2$ protons of cysteines bound to the [3Fe-4S] and [4Fe-4S] clusters. Finally, a sequential correlation between cysteines in the various proteins could be proposed through the ^{1}H NMR shifts of the β-CH$_2$ protons.

The present work shows how the experimental ^{1}H NMR data collected over the years can be rationalized in a reasonably unified picture for 3Fe-4S and 7Fe-8S classes of ferredoxins and how the differences among the classes may reflect differences in primary structures. NMR may thus become a tool to infer structural information on new systems even in the absence of sequence or, when the sequence is available, in the absence of structural data.

The observed correlation between chemical shifts of the β-CH$_2$ cysteine protons and the protein sequence could be exploited in the case of proteins with high molecular weights, containing iron$-$sulfur cluster (for instance hydrogenases, dehydrogenases, aconitases), for which the extensive investigated or conventional NMR techniques are difficult or impossible to apply.

SUPPORTING INFORMATION AVAILABLE

284 K 500 MHz 2D NOESY spectrum of the oxidized 7Fe-8S ferredoxin from *R. palustris* (Figure S1) and calculated eigenvalues for the two lowest lying energy states of Hamiltonian (1) in [3Fe-4S] clusters for different J values (Figure S2) (3 pages). Ordering information is given on any current masthead page.

REFERENCES

Aono, S., Nakamura, S., Aono, R., & Okura, I. (1994) *Biochem. Biophys. Res. Commun. 201*, 938$-$942.

Aono, S., Bertini, I., Cowan, J. A., Luchinat, C., Rosato, A., & Viezzoli, M. S. (1996) *JBIC 1*, 523$-$528.

Armstrong, F. A., George, S. J., Thomson, A. J., & Yates, M. G. (1988) *FEBS Lett. 234*, 107.

Aue, W. P., Bartholdi, E., & Ernst, R. R. (1976) *J. Chem. Phys. 64*, 2229$-$2235.

Banci, L., Bertini, I., Luchinat, C., Piccioli, M., Scozzafava, A., & Turano, P. (1989) *Inorg. Chem. 28*, 4650−4656.

Banci, L., Bertini, I., Briganti, F., Luchinat, C., Scozzafava, A., & Vicens Oliver, M. (1991) *Inorg. Chem. 30*, 4517−4524.

Banci, L., Bertini, I., Ciurli, S., Ferretti, S., Luchinat, C., & Piccioli, M. (1993) *Biochemistry 32*, 9387−9397.

Banci, L., Bertini, I., & Luchinat, C. (1994) *Methods Enzymol. 239*, 485−514.

Bartsch, R. G. (1971) *Methods Enzymol. 23*, 344−363.

Battistuzzi, G., Borsari, M., Ferretti, S., Luchinat, C., & Sola, M. (1995) *Arch. Biochem. Biophys. 320*, 149−154.

Bax, A., & Davis, D. G. (1985a) *J. Magn. Reson. 65*, 355−360.

Bax, A., & Davis, D. G. (1985b) *J. Magn. Reson. 63*, 207−213.

Beinert, H. (1990) *FASEB J. 4*, 2483−2491.

Bentrop, D., Bertini, I., Luchinat, C., Mendes, J., Piccioli, M., & Teixeira, M. (1996) *Eur. J. Biochem. 236*, 92−99.

Berg, J. M., & Holm, R. H. (1982) in *Iron−Sulfur Proteins* (Spiro, T. G., Ed.) pp 1−66, Wiley-Interscience, New York.

Bertini, I., & Luchinat, C. (1996) *Coord. Chem. Rev. 150*, 1−292.

Bertini, I., Banci, L., & Luchinat, C. (1989a) in *Nuclear Magnetic Resonance, Part B* (Oppenheimer, N. J., & James, T. L., eds.) p 246 (*Methods Enzymol. 177*), Academic Press, London.

Bertini, I., Luchinat, C., Messori, L., & Vasak, M. (1989b) *J. Am. Chem. Soc. 111*, 7300−7303.

Bertini, I., Briganti, F., Luchinat, C., Scozzafava, A., & Sola, M. (1991) *J. Am. Chem. Soc. 113*, 1237−1245.

Bertini, I., Luchinat, C., & Tarchi, D. (1993) *Chem. Phys. Lett. 203*, 445−449.

Bertini, I., Luchinat, C., Piccioli, M., & Tarchi, D. (1994) *Concepts Magn. Reson. 6*, 307−335.

Bertini, I., Ciurli, S., & Luchinat, C. (1995) *Struct. Bonding 83*, 1−54.

Bertini, I., Donaire, A., Felli, I. C., Luchinat, C., & Rosato, A. (1996) *Magn. Reson. Chem. 34*, 948−950.

Busse, S. C., La Mar, G. N., Yu, L. P., Howard, J. B., Smith, E. T., Zhou, Z. H., & Adams, M. W. W. (1992) *Biochemistry 31*, 11952−11962.

Cammack, R. (1992) *Adv. Inorg. Chem. 38*, 281−322.

Chen, Z. G., de Ropp, J. S., Hernandez, G., & La Mar, G. N. (1994) *J. Am. Chem. Soc. 116*, 8772−8783.

Cheng, H., Grohmann, K., & Sweeney, W. V. (1990) *J. Biol. Chem. 265*, 12388−12392.

Cheng, H., Grohmann, K., & Sweeney, W. V. (1992) *J. Biol. Chem. 267*, 8073−8080.

Day, E. P., Peterson, J., Bonvoisin, J. J., Moura, I., & Moura, J. J. G. (1988) *J. Biol. Chem. 263*, 3684−3689.

Donaire, A., Gorst, C. M., Zhou, Z. H., Adams, M. W. W., & La Mar, G. N. (1994) *J. Am. Chem. Soc. 116*, 6841−6849.

Dugad, L. B., La Mar, G. N., Banci, L., & Bertini, I. (1990) *Biochemistry 29*, 2263−2271.

Glenn, J. K., & Gold, M. H. (1985) *Arch. Biochem. Biophys. 242*, 329−341.

Gorst, C. M., Yeh, Y.-H., Teng, Q., Calzolai, L., Zhou, Z.-H., Adams, M. W. W., & La Mar, G. N. (1995) *Biochemistry 34*, 600−610.

Holm, R. H. (1992) *Adv. Inorg. Chem. 38*, 1−71.

Huynh, B. H., Moura, J. J. G., Moura, I., Kent, T. A., LeGall, J., Xavier, A. V., & Munck, E. (1980) *J. Biol. Chem. 255*, 3242−3244.

Johnson, M. K., Bennett, D. E., Fee, J. A., & Sweeney, W. V. (1987) *Biochim. Biophys. Acta 911*, 81−94.

Kent, T. A., Huynh, B. H., & Munk, E. (1980) *Proc. Natl. Acad. Sci. U.S.A. 77*, 6574−6576.

Kissinger, C. R., Sieker, L. C., Adman, E. T., & Jensen, L. H. (1991) *J. Mol. Biol. 219*, 693−715.

Luchinat, C., & Piccioli, M. (1995) in *NMR of Paramagnetic Macromolecules. NATO ASI Series* (La Mar, G. N., Ed.) pp 1−28, Kluwer Academic, Dordrecht.

Luchinat, C., Capozzi, F., Borsari, M., Battistuzzi, G., & Sola, M. (1994) *Biochem. Biophys. Res. Commun. 203*, 436−442.

Macedo, A. L., Moura, I., Moura, J. J. G., LeGall, J., & Huynh, B. H. (1993a) *Inorg. Chem. 32*, 1101−1105.

Macedo, A. L., Palma, P. N., Moura, I., LeGall, J., Wray, V., & Moura, J. J. G. (1993b) *Magn. Reson. Chem. 31*, S59−S67.

Macura, S., & Ernst, R. R. (1980) *Mol. Phys. 41*, 95.

Meyer, T. E., Przysiecki, C. T., Watkins, J. A., Bhattacharyya, A., Simondsen, R. P., Cusanovich, M. A., & Tollin, G. (1983) *Proc. Natl. Acad. Sci. U.S.A. 80*, 6740−6744.

Moura, I., Moura, J. J. G., Munck, E., Papaefthymiou, V., & LeGall, J. (1986) *J. Am. Chem. Soc. 108*, 349−351.

Moura, J. J. G., Xavier, A. V., Bruschi, M., & LeGall, J. (1977) *Biochim. Biophys. Acta 459*, 306−318.

Nagayama, K., & Ohmori, D. (1984) *FEBS Lett. 173*, 15−18.

Nagayama, K., Ohmori, D., Imai, Y., & Oshima, T. (1983) *FEBS Lett. 158*, 208−212.

Nagayama, K., Imai, Y., Ohmori, D., & Oshima, T. (1984) *FEBS Lett. 169*, 79−84.

Stout, C. D. (1989) *J. Mol. Biol. 205*, 545−555.

Sweeney, W. V. (1981) *J. Biol. Chem. 256*, 12222−12227.

Thomson, A. J. (1985) in *Metalloproteins* (Harrison, P., Ed.) p 79, Verlag Chemie, Weinheim.

Vold, R. L., Waugh, J. S., Klein, M. P., & Phelps, D. E. (1968) *J. Chem. Phys. 48*, 3831−3832.

Werth, M. T., Kurtz, D. M., Jr., Moura, I., & LeGall, J. (1987) *J. Am. Chem. Soc. 109*, 273−275.

Yoch, D. C., & Carithers, R. P. (1979) *Microbiol. Rev. 43*, 384.